Analysis of Hex Cap Fasteners Revealed Dimensional Related Failure Causation

by Keith Bailey

Performance of fasteners relies on several factors including the intended design load, metallurgical properties associated with a given grade and geometry. For a given size fastener, these are several grades from which an architect or engineer may select for a given load capacity. Considerations when selecting a particular fastener commonly include but are not limited to the environment, expected life, cost and more importantly the in service shear and tensile loads. Higher grade fasteners used in more critical applications where failures could result in loss of life or substantial property damage have full size test requirements. One such procedure is the wedge test discussed in ASTM F 606 "Standard Test Methods for Determining the Mechanical Properties of Externally Threaded Fasteners, Washers and Rivets". This test method in part analyzes the designed radius of curvature in the shank to head radius.

This paper discusses the metallurgical failure analysis of two L9 grade hex cap fasteners which failed to meet the requirements associated with section 3.5.1 of ASTM F 606 (Figure 1). These non-compliant test results lead to the metallurgical analysis to determine the likely cause of the failures at the radius transition between the head and shank features. This destructive metallurgical investigation included a macroexamination, fractography, chemical analysis of the base alloy, microexamination, hardness evaluation and mechanical testing.

Figure 1 Photomacrograph of the as received fasteners submitted for a destructive metallurgical examination.

Macroexamination and Fractography Analysis

Initial examination of the fractured bolts was performed with the unaided eye and employment of a stereomicroscope from 7 to 30X.

Initial examination of the submitted fasteners revealed both to exhibit plastic deformation/deflection in the shank region consistent with a wedge type test similar to that discussed in ASTM F 606 (Figure 2). Evaluation of the load bearing surface of both heads also revealed localized plastic deformation consistent with that of a wedge type mechanical test (Figures 3 and 4). Evaluation of the fracture and other regions revealed no instances consistent with manufacturing defects or surface discontinuities such as those discussed in Section 3 of SAE J 123 (Figures 5-8). These include but are not limited to the lack of fracture surface defect features such as voids, internal cracks, forging flow line re-entry, relatively large inclusions/oxides and evidence of quench cracking. This also includes but is not limited to the lack of observations of the following surface discontinuities: quench cracks, seams, bursts, shear burst, voids, laps, folds, appreciable tooling marks, significant nicks or gouges. Analysis of the failure surfaces revealed the presence of a shear lip at both the fracture initiation and final failure locations for each

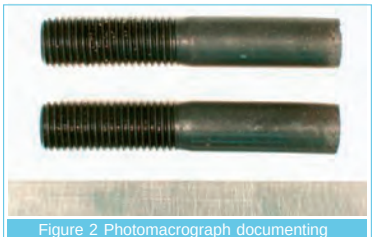

Figure 2 Photomacrograph documenting the plastic deflection observed for both fastener shank regions.

Figure 3 Photomacrograph documenting the load bearing surface for fastener A head.

Figure 4 Photomacrograph documenting the load bearing surface for fastener B head.

Figure 5 Photomacrograph documenting the fracture surface, head side, of fastener A revealing no significant evidence of internal defects.

Figure 6 Photomacrograph documenting the fracture surface, head side, of fastener B revealing no significant evidence of internal defects.

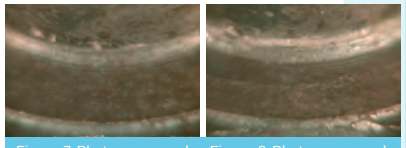

Figure 7 Photomacrograph documenting the typical surface appearance in the radius transition from the shank to head bearing surface for fastener A.

Figure 8 Photomacrograph documenting the typical surface appearance in the radius transition from the shank to head bearing surface for fastener B.

(Figures 3-6). These observations are consistent with a wedge type mechanical test.

Both fracture surfaces of each fastener were also examined at higher magnification to determine the failure mode(s). This stage of the fractography analysis was performed using a scanning electron microscope.

Results of this analysis revealed both fracture surfaces to exhibit a dimpled appearance consistent with a ductile overload associated with a wedge test (Figures 9 and 10). Evaluation of the fracture initiation regions exhibited a shear dimple pattern and no indication of an oxide film to be present which would indicate a potential quench crack defect.

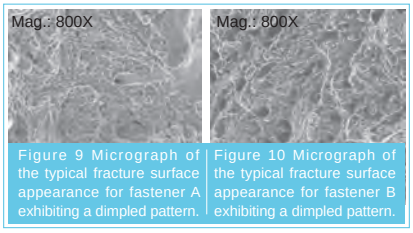

Figure 9 Micrograph of the typical fracture surface appearance for fastener A exhibiting a dimpled pattern.

Figure 10 Micrograph of the typical fracture surface appearance for fastener B exhibiting a dimpled pattern.

Each head/shank was cross sectioned with a water fed abrasive cut off saw to obtain a longitudinal cross section through the approximate fracture initiation location for flow line analysis. These cross sections were metallographically prepared in accordance with ASTM E 3.

Results of this analysis revealed the flow line of each fastener cross section to exhibit no evidence of re-entry or laps (Figures 11 and 12).

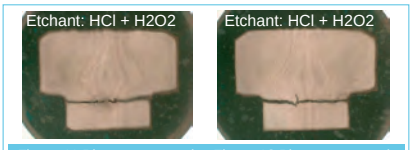

Figure 11 Photomacrograph documenting the flow lines of the cross section extracted from fastener A.

Figure 12 Photomacrograph documenting the flow lines of the cross section extracted from fastener B.

Results of this stage of the analysis concluded the fasteners to have been wedge tested and no external or exposed internal surface defects were observed which would have been attributed to the manufacturing process. Analysis of the fracture surface revealed a ductile overload type failure mode typically observed for this type and grade of fastener.

Chemical Analysis

A portion of each fastener shank was analyzed for base alloy elemental composition by Optical Emission Spectroscopy (OES) in accordance with Fed Test Standard 151B, Method 112.2. Results of this testing revealed the base alloy of both fasteners to have an elemental composition consistent with UNS G41400 (4140, Cr-Mo Alloy Steel). Results of this analysis are consistent with the base alloy requirements stated by the requestor. Results are provided in Table 1.

Element	Fastener A Base Alloy(wt%)	Fastener B Base Alloy(wt%)	Alloy Requirements of UNS G414001(wt%)
C	0.41	0.42	0.38-0.43
Cr	0.92	0.93	0.80-1.10
Mn	0.79	0.80	0.75-1.00
Mo	0.20	0.20	0.15-0.25
P	0.008	0.008	0.035 max
S	0.022	0.020	0.040 max
Si	0.26	0.26	0.15-0.35
Fe	Base	Base	Base

Table 1 Elemental composition of the submitted fastener base alloys and requirements for UNS G41400 (4140) in weight percent.

Microstructure Examination

The cross sections extracted from the submitted grade L9 fasteners and discussed in the "Macroexamination/ Fractography" section of this report were first examined in the unetched and lightly etched conditions.

Examination of both cross sections revealed no appreciable presence of an oxide layer to be present in the failure initiation regions (Figures 13 and 14). These cross sections exhibited no evidence of a significant level of precipitates/oxides in the head or shank locations. Evaluation of the cross sections in the etched condition revealed the initial fracture of the fasteners to follow the flow lines of the microstructures (Figures 15 and 16). Both fastener cross sections revealed a martensitic matrix and a small percentage of apparent ferrite (Figures 17 and 18). Evaluation of the near surface regions revealed no etch effects suggesting an appreciable level of decarburization or other alloy depletion to be present (Figures 19 and 20).

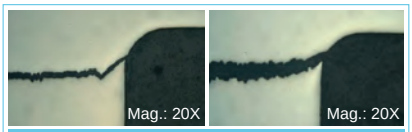

Figure 13 Photomicrograph documenting the fracture initiation region of fastener A.

Figure 14 Photomicrograph documenting the fracture initiation region of fastener B.

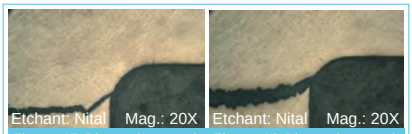

Figure 15 Photomicrograph documenting the initial fracture orientation and flow line orientation for the cross section extracted from fastener A.

Figure 16 Photomicrograph documenting the initial fracture orientation and flow line orientation for the cross section extracted from fastener B.

Figure 17 Photomicrograph documenting the martensitic microstructure observed throughout the extracted cross section of fastener A.

Figure 18 Photomicrograph documenting the martensitic microstructure observed throughout the extracted cross section of fastener B.

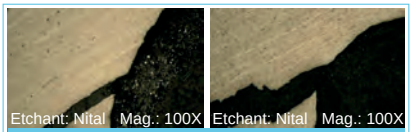

Figure 19 Photomicrograph documenting the typical near surface microstructure of fastener A exhibiting no appreciable level of alloy depletion.

Figure 20 Photomicrograph documenting the typical near surface microstructure of fastener B exhibiting no appreciable level of alloy depletion.

Results of this microexamination revealed no microstructural defects to have contributed to the fracture of the two fasteners. Analysis of the extracted cross sections revealed a typical martensitic matrix with no evidence of alloy depletion at the surface, no excessive levels of precipitates/oxides; however, the initial fracture follows the flow lines of the microstructure.

Hardness Evaluation

Microhardness testing for the extent of decarburization was performed using a Knoop indenter with a 500 gram load per ASTM E 384 per Section 3.5.1 of AMS 2759/1D. This specification was selected as it contains the most stringent requirements and the supplied drawing does not specify a particular specification for decarburization analysis. Results of this analysis are converted to HRC using Table 1 of ASTM E140. Core hardness analysis at mid radius was performed using a United True Blue Hardness Tester in accordance with ASTM E 18 per Section 3.13 of SAE J 429.

Results of this analysis revealed the near surface hardness of fastener A and B to be within 20 Knoop points of the base alloy at 0.003" and 0.004", respectively (Table 2). Results of this analysis exceed the requirements of AMS 2759/1D which states the maximum difference between the core and surface of 20 Knoop points at a maximum depth of 0.005".

Results of the mid-radius analysis revealed fasteners A and B to have an average hardness of 43 HRC and 41 HRC, respectively. Results of this evaluation revealed the mid radius regions to be within the 38-44 HRC required hardness range per customer supplied specifications.

Fastener	Depth(in.)	Hardness(HK)	Average Hardness(HK)
A	Core	466	456
"	"	452	
"	"	450	
A	0.002	421	---
"	0.003	448	---
B	Core	463	463
"	"	463	
"	"	463	
B	0.002	385	---
"	0.003	421	---
	0.004	448	---

Table 2 Microhardness test results for the core and near surface regions of fasteners A and B.

Mechanical Testing

One tensile sample was extracted from each of the fastener shank regions, machined and tested in accordance with ASTM E 8.

Results of this analysis revealed the ultimate tensile strength of fasteners A and B to be 193 ksi and 194 ksi, respectively (Table 3). Results of this analysis revealed both fastener base alloys to exceed the minimum requirements of 180 ksi per the customer supplied drawing. The yield strength, percent elongation and percent area reduction are also supplied in Table 3.

Fastener	Ultimate Tensile Strength (ksi)	Yield Strength (ksi)	Percent Elongation (%)	Percent Area Reduction (%)
A	193	180	16	43
B	194	179	15	53

Table 3 Mechanical test data obtained from machined tested bars extracted from fasteners A and B.

Conclusions

Complete metallurgical analysis of the two submitted fractured fasteners revealed the likely failure causation to be attributed to a relatively small radius of curvature at the head to shank transition. Marco and microexamination of the fastener surfaces and cross sections revealed no appreciable defects which would have contributed to the failure in the head to shank transition. Analysis of the fracture surface revealed a ductile overload type failure mode typically observed for this type and grade of fastener. Chemical analysis revealed the base alloy of both fasteners to meet the compositional requirements specified by the customer. Analysis of the extracted cross sections revealed a typical martensitic matrix typically observed for this type of alloy and grade. Hardness evaluation revealed no appreciable surface decarburization to be present on either fastener. Core hardness testing revealed both to adhere to the customer specified range. Mechanical testing revealed the ultimate tensile strength of fasteners A and B to meet the minimum required 180 ksi magnitude.

Discussions with the supplier revealed a change in the radius of the head to shank transition reduced the failure rate in this region to zero. Based on this information and results of the metallurgical evaluation of the two fasteners it is determined the observed failure location to be attributed to the geometrical design of a relatively small radius of curvature in this feature.